

## Quantitative Imaging of Alveolar Recruitment with Hyperpolarized Gas MRI

M. F. Cereda<sup>1</sup>, K. Emami<sup>2</sup>, S. J. Kadlec<sup>2</sup>, Y. Xin<sup>2</sup>, P. Mongkolwisetwara<sup>2</sup>, H. Profka<sup>2</sup>, A. Barulic<sup>2</sup>, S. Pickup<sup>2</sup>, N. N. Kuzma<sup>2</sup>, M. Ishii<sup>3</sup>, H. Hamedani<sup>2</sup>, B. M. Pullinger<sup>2</sup>, R. Ghosh<sup>2</sup>, J. Rajaei<sup>2</sup>, C. S. Deutschman<sup>1</sup>, and R. R. Rizi<sup>2</sup>

<sup>1</sup>Anesthesiology and Critical Care, University of Pennsylvania, Philadelphia, Pennsylvania, United States, <sup>2</sup>Radiology, University of Pennsylvania, Philadelphia, Pennsylvania, United States, <sup>3</sup>Otolaryngology-Head & Neck Surgery, Johns Hopkins University, Baltimore, Maryland, United States

**INTRODUCTION:** Hyperpolarized (HP) gas MRI allows to measure the apparent diffusion coefficient (ADC) of <sup>3</sup>He within the acinar airspaces, including the alveoli and the respiratory bronchioles. Measurements of <sup>3</sup>He ADC have been shown to be sensitive to changes in alveolar size caused by pulmonary diseases such as emphysema and interstitial fibrosis. <sup>3</sup>He HP MRI may also help to assess the effects of atelectasis on alveolar mechanics and geometry in mechanically ventilated subjects. The information provided by this technique could help elucidate the mechanisms through which atelectasis promotes iatrogenic lung injury during mechanical ventilation. In addition, the effects of alveolar recruitment maneuvers on lung micromechanics could be better characterized by localized ADC measurements. In this work, we utilized HP gas diffusion MRI to test the hypothesis that atelectasis causes pathological airspace overdistension and that this abnormal pattern of lung inflation is reversed by the application of alveolar recruitment maneuvers.

**METHODS:** Healthy male Sprague-Dawley rats ( $n=10$ , BW=250±50g) were anesthetized with pentobarbital, temporarily paralyzed with pancuronium, intubated, and mechanically ventilated by a custom small-animal MR-compatible ventilator with a delivery accuracy of ±100µL/breath. Rats were breathing a mixture of <sup>4</sup>He:O<sub>2</sub> (4:1) at 60 BPM and I:E=1:2, at a nominal  $V_T=10\text{ml/kg}$ . The animal's peak inspiratory pressure (PIP) was continuously monitored and recorded by a high-precision MR-compatible optical pressure transducer (Samba Sensors AB). For ADC imaging rats were ventilated with five identical breaths of HP <sup>3</sup>He:O<sub>2</sub> (4:1) at the designated PEEP level followed by a 3-sec breath-hold during which five diffusion-weighted images were acquired corresponding to  $b$ -values = 0.00, 3.73, 2.18, 1.00 and 0.00  $\text{s}/\text{cm}^2$ . This procedure was repeated immediately with identical but reversed polarity diffusion gradient  $b$ -values. These 10 diffusion-weighted images were then combined to yield the ADC map of the imaged slice according to a double-acquisition diffusion imaging scheme described earlier [1]. Images were acquired using a diffusion-weighted gradient echo imaging pulse sequence with centric phase-encoding in a 50-cm bore 4.7-T MRI scanner (Varian Inc) equipped with a 12-cm, 25-G/cm gradients and a 2-3/4"-ID quadrature 8-leg birdcage body coil (Stark Contrast). Images were acquired in the middle coronal slice of the rat lung with the following imaging parameters: FOV=6x6cm<sup>2</sup>, ST=6mm, MS=64x64,  $\alpha=4\text{--}5^\circ$ , TR=6.6ms, and TE=4ms. Diffusion sensitizing gradient was applied along the phase-encoding (L-R) direction with the following timing parameters:  $\Delta=1\text{ms}$ ,  $\delta=200\mu\text{s}$ , and  $\tau=180\mu\text{s}$  according to the naming convention of [2]. After the initial preparatory period (minimum of 1 hr), an alveolar recruitment maneuver was performed by a transient application of PEEP 9 cmH<sub>2</sub>O with constant TV. The maneuver was followed by a wait period of variable duration (8–44 min) at zero PEEP, following which a second recruitment maneuver was performed in an identical manner to the first one. ADC measurement was performed at four time points corresponding to immediately before (panels I, III) and after (panels II, IV) each of the two recruitment maneuvers, as shown in Figure 1. For each measurement, mean ADC values, standard deviations, and skewness values of the distribution were calculated. Three additional animals were used exclusively for the measurement of airway pressures and received a recruitment maneuver after a one-hour wait period at zero PEEP.

**RESULTS AND DISCUSSION:** An hour of ventilation at zero PEEP had likely caused a non-negligible degree of atelectasis that was re-expanded by subsequent recruitment maneuvers. This re-expansion, evidenced by the recorded PIP reduction (an indicator of improved lung compliance), was observed in 3 animals after a recruitment maneuver ( $-32.7\pm8.5\% [P<0.05, n=3]$ ). ADC maps, as shown in Figure 1, demonstrated a shift in ADC distributions to lower values after each recruitment maneuver, suggesting a decrease in individual sizes of ventilated acinar airspaces induced by additional alveolar recruitment (where the same tidal volume is distributed across more alveoli, reducing the distension of individual alveoli). During the wait period between the two maneuvers at zero PEEP, ADC was observed to increase towards higher values. Statistical analysis revealed a significant decrease in the mean ADC after each recruitment maneuver, as shown in Figure 2. The increase in ADC between maneuvers was also statistically significant and was time-dependent, as suggested by its correlation with the duration of the wait period ( $r=0.66$ ). The relative change in ADC after the second maneuver was smaller than after the first one, which was likely due to differences in the duration of the wait periods. We did not observe a statistically significant effect of recruitment maneuvers on ADC dispersion, as measured by the ADC standard deviation of each image, also shown in Figure 2. However, the skewness of ADC distribution was significantly shifted to the left after the first maneuver, which suggests the recruitment of smaller alveolar units. Our findings suggest that atelectasis causes a redistribution of inspired gas from atelectatic alveoli to airspaces that remain ventilated, which become relatively overdistended. Alveolar recruitment maneuvers reestablish a normal pattern of alveolar distension, probably by reopening collapsed alveoli and allowing the redistribution of inspired volume to a larger number of ventilated alveoli.

**CONCLUSION:** Results of this study suggest that atelectasis causes overdistension of ventilated airspaces. This phenomenon could be one of the mechanisms through which atelectasis contributes to lung injury during mechanical ventilation, as suggested by animal studies. HP <sup>3</sup>He diffusion MRI provides a unique opportunity to evaluate the microstructural effects of mechanical ventilation at the level of alveoli and other acinar airspaces. This information is relevant since it is the alveolar response to mechanical ventilation that triggers the iatrogenic lung injury. This technique can be applied to other models of lung injury, such as surfactant deficiency and sepsis, to characterize the response of alveolar micromechanics to mechanical ventilation in the presence of abnormal pulmonary pathophysiology.

**REFERENCES:** [1] Emami, K, et al. Proc Int Soc Mag Reson Med 2007; [2] Yu, J, et al. J Magn Res Imag 2007.

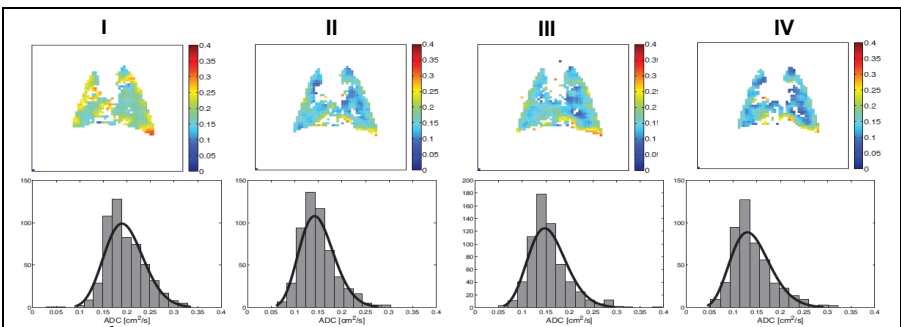


**Figure 1:** <sup>3</sup>He ADC maps and frequency distributions measured before (I, III) and after (II, IV) two consecutive recruitment maneuvers, separated by a wait time period.

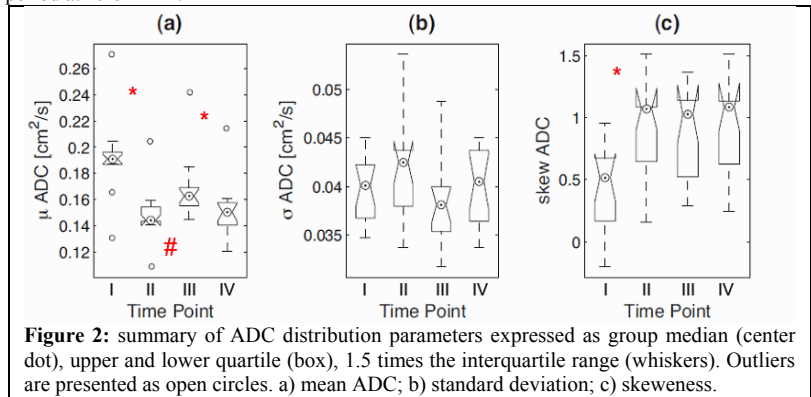


**Figure 2:** summary of ADC distribution parameters expressed as group median (center dot), upper and lower quartile (box), 1.5 times the interquartile range (whiskers). Outliers are presented as open circles. a) mean ADC; b) standard deviation; c) skewness.

\*:  $p<0.01$  1 vs. 2 and 3 vs. 4; #:  $p<0.01$  2 vs. 3.